Evaluation of Selected 3D Data Acquisition Systems for Capturing the Geometry of Building Structures

Richard Honti, Ján Erdélyi and Tomáš Funtík

Slovak University of Technology in Bratislava, Faculty of Civil Engineering, Radlinského 2766/11, 810 05 Bratislava, Slovakia
richard.honti@stuba.sk, jan.erdelyi@stuba.sk, tomas.funtik@stuba.sk

Abstract: Accurate 3D data from indoor environments are highly important for various applications in construction, indoor navigation, and real estate management. Mobile scanning systems (simultaneous localization and mapping (SLAM), mobile devices with LIDAR) and modern systems, such as Matterport offer an efficient way to produce virtual models of the measured objects (or even generate point clouds). Still, the quality of these methods tends to be lower than the quality of the measurements performed by terrestrial laser scanning (TLS). In this paper, three distinct scanning systems are compared and evaluated. The tested techniques are the Matterport-generated virtual models using 360° photos, the Matterport PRO3 LIDAR camera and point clouds from the SLAM handheld scanner GeoSLAM ZebGO. The evaluation is done against the survey-grade TLS point clouds captured from four test sites with different properties (e.g., size, complexity, etc.). The selected test scenes are indoor environments, including a hallway, an office, a measurement laboratory, and a lecture hall. Their strengths and weaknesses, from both technical and practical perspectives are shown, which can assist in selecting the most appropriate system for different applications.

Keywords: data acquisition; TLS; LIDAR; SLAM; Matterport

1 Introduction

The architectural and building industry continually evolves, driven by the high demands for efficient and innovative technologies and solutions. In this context, the need for accurate documentation of building structures has a high justification since these data can be the foundation for decision-making, structural analysis, the creation of accurate 3D models (e.g., building information models (BIM)) with great detail, and many more. Using innovative techniques for data capturing and the development of information technologies brings significant progress in the digitalization of the building industry. It allows automation (at some level) of all the processes throughout the building's whole lifecycle.

Conventional field measurements in the case of more extensive and complex buildings or objects can be labor-intensive, time-consuming, and inefficient, requiring a considerable number of measurements. So, these methods primarily do not meet the requirements for automating the building industry's digitization processes. However, in the last decade, huge improvements have been made in 3D data acquisition methods with the development of surveying and mapping technologies. The need for 3D measurements, accurate 3D information is rapidly increasing in all related fields, such as digitization or 3D modeling of the built environment [1], BIM modeling (Scan-to-BIM) [2] [3], geometry check of building structures with the Scan-vs-BIM methodology [4] [5], reverse engineering [6], cultural heritage documentation and preservation and others. That is because 3D visualization provides a better understanding and multiple possibilities for different analyses [7]. In most cases, the raw basis of 3D models of any kind is a point cloud. Several 3D data acquisition techniques can be used for capturing and digitization of the geometry of real-world objects. The most used techniques are terrestrial laser scanning (TLS), close-range photogrammetry (or 360° photogrammetry), SLAM (Simultaneous Localization And Mapping) enabled handheld scanning systems, and mobile devices with LIDAR sensors. Terrestrial laser scanners generate point clouds with high accuracy and relatively low levels of noise compared to the other techniques. However, the data acquisition can be more time-consuming and, in some cases, requires careful planning. This is true, especially in the case of indoor environments, where the number of needed scanning stations is raised since the indoor space is divided into rooms, corridors, stairs, and other facilities with varied shapes and functions. Besides that, the number of instrument positions is also raised by the limited visibility of the measured objects. Limited visibility means these measured spaces are mostly not empty (e.g., furniture, interior fittings, etc.). In contrast, SLAM-enabled mobile laser scanners (MLS), methods like Matterport, or mobile devices with LIDAR sensors offer the possibility to measure the geometry of the object quicker and more efficiently, however, to achieve a certain level of accuracy of the final point cloud can be challenging and complicated.

The result from the mentioned techniques can be a point cloud that will be the subject of the evaluation. The exception is Matterport, where the direct result of the 3D capturing is a virtual photogrammetric model (or a mesh model), regardless of what type of sensor is used for the data acquisition. However, suppose the measurement is executed using the selected sensors (e.g., Matterport Pro3 LIDAR camera, Matterport Pro2 camera, or Leica BLK360 scanner); high-density point clouds can also be generated from these virtual models. In addition, measurement (derivation of the dimensions and the geometry of objects) can also be performed on virtual models from Matterport.

There are several approaches for point cloud evaluation; in general, they can be divided into three main categories [8]: control point approach, approach based on a comparison of the segmented parts of the point cloud, and cloud-to-cloud approach. The first, the control point approach, consists of manually selecting two control

points in some selected characteristic parts of the object, e.g., features like corner points of some building structures, building openings, etc. Then, the Euclidean distances between these points can be calculated and compared between several point clouds. Jung et al. [9] used total stations to measure the coordinates of the selected control points. Then, they calculated the Euclidean distances between them and compared them to the exact distances obtained from the points clouds concerning BIM standards [8]. In the case of the second category, first, subsets of points are segmented from the point clouds. Then, the evaluation (several analyses, e.g., object deformation) is done on these subsets. This method is more complicated than the first one but gives more "freedom" (possibilities for analysis or evaluation). Simacek et al. [10] compared the point clouds from two instruments (ZEB1 and Leica C10 laser scanner) for indoor scanning. They performed a quantitative analysis by comparing local point density, local noise level, and stability of local normal vectors. Firstly, they segmented the walls from both point clouds and separately compared the parameters mentioned on each wall's point clouds. They also generated a simple 3D room plan and compared the dimensions of the constructed line segments of the room. The third is the cloud-to-cloud approach, where the chosen metrics are calculated between two whole point clouds. It is clear that this method is the most complicated, and it can be time-consuming. However, it is the most robust of the listed methods. The most significant advantage of this method is that the whole surface of the measured object is compared, so it can also provide a complex model of the object's deformations caused by the "distortion" of the collected data. It is also often applied for deformation monitoring using point clouds measured with TLS. In this paper, all three approaches are used. The first approach is necessary since the Matterport models, collected using 360° cameras, do not allow the creation of high-density point clouds. The latter two approaches are used for scanning techniques capable of generating a high-density point cloud.

2 Selected 3D Data Acquisition Techniques

Several novel 3D data acquisition systems have been introduced in the last decade for digitizing indoor spaces of buildings. However, the usability and accuracy of these methods have not been thoroughly investigated before. This paper examines this issue by comparing the results from the selected systems with the survey-grade TLS. Some of the most used systems were chosen for evaluation: Matterport's system using 360° cameras, the Matterport Pro3 LIDAR camera, and the SLAM-enabled handheld laser scanner GeoSLAM ZebGO.

The reference data was captured by terrestrial laser scanning to evaluate the point clouds (or results) generated from the mentioned data acquisition techniques. Terrestrial laser scanning systems are contactless measuring techniques, enabling the determination of 3D coordinates of points with a survey-grade accuracy on the measured object's surface by emitting laser pulses toward this object.

The fundamental operating principle of most laser scanners is the space polar method. In this method, the 3D position of each point is determined based on the measured horizontal and vertical angles, along with the measured length [11].

2.2 Matterport

The first data acquisition system to be evaluated in this paper is Matterport, a commercial indoor mapping system. It was selected because it provides a cost-effective alternative for indoor mapping. In general, this technology does not require complicated planning for the field measurement, and it can be faster and more efficient than TLS. Matterport is a 3D camera system that can capture real-world objects and create a digital photogrammetric model of buildings, interiors, or other environments. Generally, this system uses two data types to create the digital model of a measured space: images and depth maps. Images are used to visualize the measured object, and depth maps are used to estimate the distance between the sensor position for capturing and the points on the object's surface [12]. This information is then used to generate a 3D model. To address this task, Matterport's Cortex artificial intelligence is employed [13]. Cortex AI is a deep learning neural network capable of generating 3D data from a variety of capture devices, including LIDAR systems, 360° cameras, and smartphones.

The whole measurement is controlled via the Matterport mobile application. Then, after the measurement, the scans are uploaded to the Matterport cloud for processing to create a 3D photogrammetric virtual model. Two different sensors were selected for this system: a readily available and affordable 360° camera (Ricoh Theta Z1) and the Matterport Pro3 LIDAR camera, developed by Matterport itself.

2.2.1 Matterport with 360° Camera

In this case, the selected sensor for capturing is the Ricoh Theta Z1 360° camera (Figure 1, left), which is the manufacturer's flagship model, and Matterport itself recommends it for the highest quality 360° capture. The Ricoh Theta family of cameras contains two CMOS sensors that use wide field-of-view lenses to capture two hemispheres of the environment. The sensor images share a small overlapping region stitched together to create a single panoramic image. The significant advantage of the Z1 model is that the images can be captured in RAW format with minimal image processing [14]. The camera has a 1.0-inch (25.4 mm) back-illuminated CMOS image sensor with an output pixel of approximately 23MP (6720x3360) effective megapixels. It supports RAW format with a resolution of 7296 × 3648 pixels; in the JPEG format, the resolution is 6720 × 3360 pixels. The camera has a 1" (25.4 mm) OLED information display, with 128 × 36 pixels resolution. The dimensions of the camera are 48mm (W) x 132.5mm (H) x 29.7mm (D), and it weighs approximately 182g, which makes it a very compact camera.

The disadvantage of using a 360° camera within the Matterport system is that it is not possible to generate high-density point clouds from the captured model; the result of the measurement is a 3D virtual photogrammetric model in the Matterport application.

Figure 1
Ricoh Theta Z1 (left) and the Matterport Pro3 Lidar camera (right)

2.2.2 Matterport with Pro3 LIDAR Camera

The second apparatus is the Matterport's LIDAR camera, the Matterport Pro3 (Figure 1 right), which was introduced in August 2022. The device is equipped with a LIDAR depth sensor with laser class 1 (wavelength of 904 nm) and one 20 MP imaging sensor with a 12-element lens covering an ultra-wide angle. The dimensions of the camera are 181mm (W) x 161.4 mm (H) x76 mm (D) with weight of 2.2 kg. The field of view of the LIDAR sensor is 360° in horizontal and 295° in vertical direction, with accuracy of ±20 mm at 10 m distance. The operating range is from 0.5 m up to 100 m. The scanning speed achieves 100,000 points per second (1,5 million points per scan), and one whole scan is completed in less than 20 seconds. The entire panorama image is captured from four camera positions with 134.2 MP. The huge advantage of the Matterport Pro3 camera is that it enables the generation of a high-density point cloud from the created digital photogrammetric mesh model.

2.3 GeoSLAM ZebGO

The GeoSLAM ZebGO is a SLAM-enabled handheld scanner that uses a LIDAR sensor (with laser Class 1, wavelength 905 nm) for range measurements, with a scanning range of up to 30 m in optimal conditions and a field of view of 360° x 270°. It captures 43000 points per second. The scan range noise is ±30 mm, according to the manufacturer. The handheld scanner (Figure 2 - right) weighs 0.95 kg, and the datalogger (incl. battery) weighs 1.70 kg. An additional ZEB Cam camera is needed for colorized point clouds. The scanning principle is that the ZebGO consists of a 2D time-of-flight LIDAR, which is coupled to an inertial

measurement unit mounted on a motor drive, and the motion of the scanning head provides the third dimension, which is required to generate the 3D data [15]. It captures the raw laser range measurements and inertial data during the scanning, which is then converted into a 3D point cloud in post-processing using the GeoSLAM's SLAM algorithm. The algorithm combines the 2D laser scan data with the inertial data to generate 3D point clouds [15].

The disadvantage of this system is that it is not possible to check the partial results during the scanning process. Therefore, some planning is needed to understand the measured environment. Also, proper scanner handling is necessary since certain principles (described in detail in the user guide [15]) must be followed to achieve the expected results.

Figure 2
GeoSLAM ZebGO

Figure 2 on the left shows all the components needed for scanning with the GeoSLAM ZebGO, battery, scanner, and connecting cable. Figure 2 on the right illustrates the scanner in more detail.

3 Test Data Characteristics and Data Acquisition

Four building spaces were selected to evaluate the data acquisition systems described in Section 2, which differ in size, complexity, shape, geometric arrangement, and density of objects (e.g., furniture). All four test scenes are located in the building of the Faculty of Civil Engineering, Slovak University of Technology in Bratislava.

The reference data was captured using a Trimble TX5 3D laser scanner with a ranging error of ±2 mm at a 25 m distance and with a range of 0.6 m – 120 m. The scanning resolution in the case of all four building scenes was set as 7.7 mm at a 10m distance. In each case, the maximum distance between the scanner and the measured object was below 15 m. The distance between the individual scanner stations varied from 5 to 7 m. The scan registration was carried out based on the overlapping areas between the point clouds from several stations in Leica Cyclone

(Version 2023.1.0) software. Additional detailed information for the test scenes is described in the following subsections.

3.1 The First Test Scene: Laboratory of Surveying

An oblong room with a repeating geometric structure, which serves as a Laboratory of Surveying in the main building of the FCE SUT in Bratislava, was selected as the first test scene. The dimensions of the laboratory are approximately 29.5 m (length) x 9.8 m (width) x 3.6 m (height). The reference point cloud captured with TLS is shown in Figure 3. A repeating structure divided by columns creates the laboratory's geometry and contains window openings on both sides. The test scene contains objects of multiple different scales. The scanning with TLS was performed from 11 different positions, as shown in the left side of Figure 3 (the empty circles on the floor mark the positions of the scanner).

Figure 3
Point cloud of the first test scene from perspective (left) and orthographic top view (right)

3.1.1 Data Acquisition with Matterport of the First Test Scene

The measurement with Matterport was carried out in two stages. In the first stage, the capturing was performed using the 360° camera, and in the second stage, with the LIDAR camera Matterport Pro3. In both cases, the measurement was repeated three times with different distances between the camera positions, which were as follows: approximately 5 m between the positions, 3 m, and 1.5 m. Figure 4 shows the instrument positions with the Pro3 camera for the first test scene.

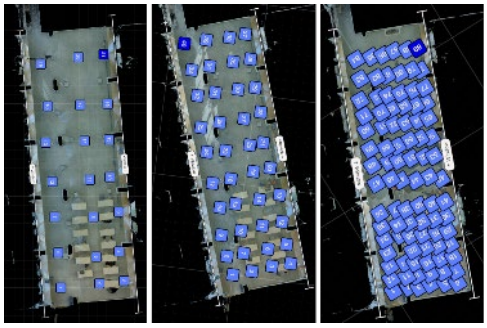

Figure 4
Positions of the instrument with Matterport Pro3 camera for the first test scene with an approximate distance between the positions: 5 m (left), 3 m (middle), 1.5 m (right)

Regarding the measurement process, in the case of the data capturing with the 360° camera with bigger distances (5 m and 3 m) between the stations, several stations had to be repeated, or a slight change of the position was needed so that the Matterport app could perform the mutual orientation of the captured photos. In addition, in some cases, the number of stations also needs to be increased due to the correct alignment of the captured photos. In the case of measurement using a LIDAR camera, such problems did not occur. Details of the measurement, such as the number of positions and the duration of the whole scanning process, are summarized in Table 1.

3.1.2 Data Acquisition with GeoSLAM ZebGO of the First Test Scene

Figure 5 shows the trajectory (red line) during the scanning with the ZebGO in the case of the first test scene. A total of 12 loops were created during the scanning since it is recommended to close the measurement loop as often as possible to minimize the error and improve the accuracy of the resulting point cloud. The measurement details are listed in Table 1.

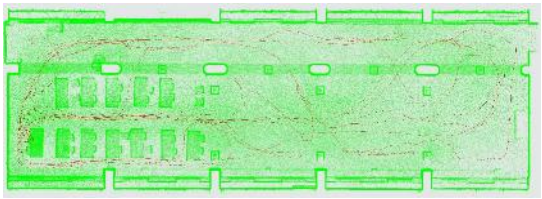

Figure 5
Orthographic top view of the acquired point cloud and the trajectory from the GeoSLAM ZebGO for the first test scene

3.2 The Second Test Scene: Hallway

A long hallway with a repeating geometric structure was selected for the second test scene. The dimensions of the hallway are 42.2 m (D) x 3.2 m (W) x 3.6 m (H), with windows on one side of the hallway.

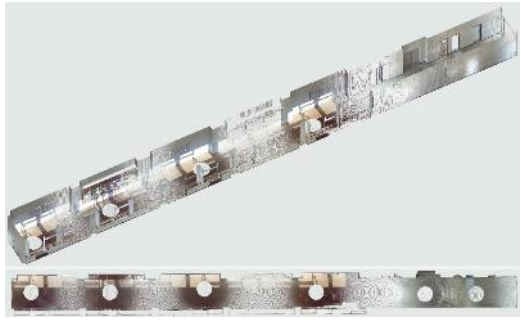

Figure 6
Point cloud of the long hallway in perspective (top) and orthographic top view (bottom)

The reference point cloud from the TLS measurement is shown in Figure 6. The scanning was performed from 6 stations.

3.2.1 Data Acquisition with Matterport of the Second Test Scene

The data acquisition with Matterport was performed in the same way as in the case of the first test scene (with 1.5 m, 3 m, and 5 m distances), described in detail in 3.1.1. The details from the measurement are summarized in Table 1.

3.2.2 Data Acquisition with GeoSLAM ZebGO of the Second Test Scene

For the second test scene, the measurement's trajectory was performed as a link from one end of the hallway to the other in ten loops with a total measurement time of 10 minutes.

3.3 The Third Test Scene: An Office

An office was selected as the third test scene with dimensions of 6.9 m (D) x 2.5 m (W) x 3.6 m (H). The office contains a lot of furniture on both sides, other objects of different scales, and a window. The reference point cloud from a perspective view and the orthographic top view are shown in Figure 7. The scanning with TLS was performed from 4 positions.

Figure 7
The reference point cloud of the third test scene from TLS (left) and the orthographic top view (right)

3.3.1 Data Acquisition with Matterport of the Third Test Scene

The Matterport system's measurement process was performed as described in Section 3.1.1 (with 1.5 m, 3 m, and 5 m distances). The details regarding the measurement are recapped in Table 1.

3.3.2 Data Acquisition with GeoSLAM ZebGO of the Third Test Scene

The scanning of the office of smaller size (test scene 3) with the GeoSLAM ZebGO was performed with straight trajectory from one side of the room to the other side in four loops, which was necessary due to the smaller size but increased geometric complexity because of the furniture and the objects located in the office.

3.4 The Fourth Test Scene: A Lecture Hall

The last test scene was a lecture hall with rectangular geometry and a stepped structure on which desks were placed. The dimensions of the lecture hall are 14.2 m (W) x 11.8 m (D) x from 4.0 to 7.0 m (H). The point cloud from the TLS measurement is shown in Figure 8. The TLS scanning was performed from 6 positions.

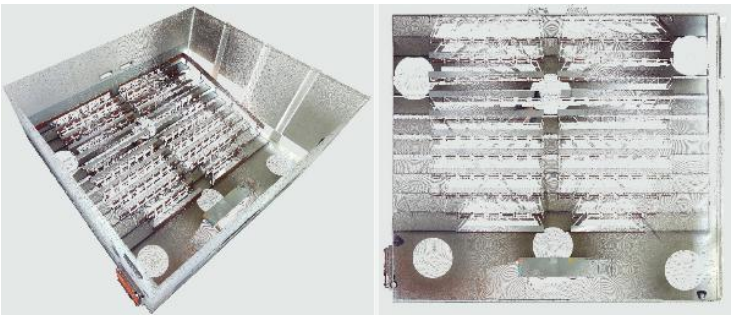

Figure 8
The reference point cloud of the fourth test scene in perspective view (left) and from an orthographic top view (right)

3.4.1 Data Acquisition with Matterport of the Fourth Test Scene

The capturing of the last test scene was also performed similarly to the methodology described in 3.1.1; however, in both cases (using the 360° camera and the Pro3 LIDAR camera), the number of measurements was reduced. Capturing with approximately 5 m and 3 m distance between the camera positions was executed, the measurement details are listed in Table 1.

3.4.2 Data Acquisition with GeoSLAM ZebGO of the Fourth Test Scene

In this case, 15 loops were created because of the stepped structure and the complex geometry on the side part of the room.

Table 1 compares the basic measurement details for each system studied in this paper and for all four test scenes, where the number of positions and the time needed (*t*) for the measurement process are listed. In the case of the Matterport system, the parameters for each measurement are described, first for the capturing with 5 m, then with 3 m, and lastly with a 1.5 m distance between the instrument positions.

Table 1
Comparison of the measurement details

	Test scene 1 (Laboratory of Surveying)		**Test scene 2 (Hallway)**		**Test scene 3 (Office)**		**Test scene 4 (Lecture Hall)**	
	stations	t [min]	stations	t [min]	stations	t [min]	stations	t [min]
M 360°*	23/43/92	12/22/35	12/18/32	6/8/13	2/4/8	1/1/3	28/60	12/25
M Pro3*	21/40/29	18/46/67	11/15/25	6/13/22	2/4/8	1/2.5/5	26/47	21/38
ZebGO	12 loops	20	10 loops	10	3 loops	5	15 loops	25
TLS (ref.)	11	40	6	25	4	10	20	60

* M 360° - Matterport system with the 360° camera, M Pro3 – Matterport system with the Pro3 LIDAR camera.

Table 2
Comparison of the basic features of individual systems

Criteria	TLS	MLS (ZebGO)	Matterport (360°)	Matterport (Pro3)
Advantages	High accuracy, long range, robust detail	Portable, quick, handles complex interiors	Easy to use, fast, low cost, available online	LiDAR, better range than 360°, available online
Limitations	Expensive, slower, requires expertise	Lower accuracy, indoor, limited range	Subscription model, no range data, lower accuracy	Subscription model, less accurate than TLS
Costs	High	Moderate	Low	Moderate/Low
Time	High	Low	Low	Moderate
Use Cases	Engineering, heritage, geospatial survey, BIM	Construction, indoor mapping, BIM	Real estate, interior design	BIM, construction, indoor scans

Table 2 compares the basic features of the evaluated systems. In the next section, the evaluation of the results from each data acquisition technique is described by comparing it with the results from the survey-grade TLS method.

4 Evaluation of the Selected Data Capturing Systems

The evaluation of the results from the studied scanning systems by comparing them with the survey-grade TLS was done using three approaches described in Section 1. Firstly, the control point approach was deployed (Section 4.1). Then, the method based on a comparison of the segmented parts of the point cloud (Section 4.2), and lastly, the cloud-to-cloud (Section 4.3) approach was used.

4.1 Control Point Approach Evaluation

In the first approach, several pairs of control points were selected between the characteristic corners in the test area (e. g., window opening, corners of building structures, etc.), and the Euclidean distance was determined between these point pairs. Firstly, these distances were measured in the reference point cloud obtained by TLS. Before the measurement, to achieve the highest measurement accuracy, the selected corner points were modeled as the intersection of three perpendicular planes in the close surroundings of the chosen corners, and the distances were measured between these modeled points. For each test scene, at least ten control point pairs were selected in the models from different parts of the test scene, and these represent parts of various objects of varying size, orientation, color, material, etc. To the Euclidean distance comparison, in addition, an indicator (*RMS – Root Mean Square)* for evaluation is defined as:

$$RMS = \sqrt{\frac{\sum_{i=1}^{n} \Delta^2}{n}} \quad (1)$$

where the Δ symbolizes the differences between the distance derived from the model resulting from TLS and the distances measured in the data obtained by the tested systems.

In the case of the Matterport models, the distances were measured directly in the Matterport app using the measuring tool available. In the case of the ZebGO scanner, the distances were calculated in the collected point cloud.

4.1.1 Evaluation of the Models Obtained by Matterport and the 360° Camera

Firstly, the Matterport system with the 360° camera was evaluated. The result of the measurement was 11 different models. For the first three test scenes (Laboratory of Surveying, Hallway, Office), three models were created with sensor positions spaced at 5 m, 3 m, and 1.5 m intervals. For the fourth test scene (Lecture Hall), two models were generated with sensor positions separated by 5 m and 3 m distances.

Table 3 shows the comparison for all the test scenes. The range of the distance differences between the TLS and the Matterport models (Table 3 middle column) and the RMS of the differences for each model are listed. The average RMS for the model with 1.5m spacing between the neighboring positions is **115 mm**. For the model with 3m spacing, it is **121 mm;** for model with 5m spacing, it is **149 mm**. The worst results were achieved in the first test scene (Laboratory of Surveying), which may be due to the size, variety, and complexity of this scene.

Table 3
Control point approach evaluation of the Matterport models captured with the 360°camera

	spacing	Differences from ® to [mm]	RMS [mm]
Test scene 1	**1.5 m**	-137 ® 278	**187**
	3 m	-157 ® 358	**221**
	5 m	-187 ® 413	**230**
Test scene 2	**1.5 m**	-8 ® 77	**41**
	3 m	-125 ® 159	**89**
	5 m	-145 ® 189	**94**
Test scene 3	**1.5 m**	8 ® 220	**116**
	3 m	-76 ® 247	**110**
	5 m	28 ® 306	**171**
Test scene 4	**3 m**	-92 ® 131	**64**
	5 m	-132 ® 211	**99**

4.1.2 Evaluation of the Models Obtained by Matterport and the Pro3 LIDAR Camera

Next, the Matterport models captured with the Pro3 LIDAR camera were evaluated. The evaluation was done in the same way, for the same point pairs as in the case of the models captured with the 360° camera. Also, multiple models were captured for each test scene with different distances between the camera positions, as described in the previous subsection. The differences between the TLS and the captured Matterport models were always below 24 mm, confirming the manufacturer's accuracy. The RMS error was always below **16 mm**.

Table 4
Control point approach evaluation of the Matterport models captured with the Pro3 camera

	spacing	Differences from ® to [mm]	RMS [mm]
Test scene 1	**1.5 m**	-16 ® 18	**12**
	3 m	-16 ® 21	**13**
	5 m	-16 ® 21	**14**
Test scene 2	**1.5 m**	-23 ® 17	**12**
	3 m	-23 ® 17	**15**
	5 m	-23 ® 17	**16**
Test scene 3	**1.5 m**	-4 ® 19	**11**
	3 m	-4 ® 19	**11**
	5 m	-4 ® 19	**12**
Test scene 4	**3 m**	-12 ® 23	**11**
	5 m	-12 ® 23	**11**

As seen in Table 4, in the case of the Pro3 camera, the differences between the models with different spacing between the positions are negligible. This can be justified by the fact that the mentioned camera has a built-in LIDAR sensor that directly measures the distances between the camera and the objects measured during the measurement.

4.1.3 Evaluation of the ZebGO-handheld Scanner Results

The last system evaluated is the handheld scanner GeoSLAM ZebGO, where the direct result from the measurement is a point cloud. Also, in this case, the comparison was made at the exact Euclidean distances between the same control point pairs of the objects. Table 5 shows the characteristics of the control point approach evaluation. The average RMS error for this system reaches **22 mm**.

Table 5
Control point approach evaluation of the point clouds captured with the ZebGO scanner

	Differences from ® to [mm]	RMS [mm]
Test scene 1	-3 ® 35	**26**
Test scene 2	-26 ® 30	**20**
Test scene 3	-31 ® 21	**18**
Test scene 4	-10 ® 40	**24**

4.2 Segmentation-based Evaluation

The second approach of the evaluation is based on comparing the point cloud segmentation results for several building elements. The Matterport system with the 360° camera was excluded from the comparison since generating a high-density point cloud from these models is not possible. Firstly, for comparison, planar sections were segmented from each point cloud using the algorithm described in [16], where the threshold parameters of the segmentation were always the same for each model. Orthogonal regression is used for plane estimation, where the best-fit regression plane is calculated by minimizing its orthogonal distances from the resulting plane [16]. The segmentation process was repeated ten times for all the models obtained by the capturing systems, and the segmented clouds with the best results were used for comparison. The segmentation of other parts (e.g., the column detail) was done manually.

Figure 10 shows the segmentation results for some of the selected key objects. A wall segment (*Wall, Wall detail*) is compared between the three systems in the first and the second row. In the third row, a detail of the edge of a planar surface of the column fronts between the window openings (*Edge detail*), and in the fourth row, a segmented column is shown (*Column detail*). Figure 10 illustrates the sharpness of the spatial geometrical details and the potential for identifying the edges and details of the presented objects. From the visual inspection, the coarse features (e.g., larger walls) are clearly visible and identifiable in the point clouds from all three methods. Smaller objects (e.g., a whiteboard hanging on a wall) are recognizable from the Pro3 model (however, the edges are not clearly identifiable) but are already challenging to identify in the case of the ZebGO. Finer features, such as a clock hanging on a wall (Figure 10 – Wall detail) or electrical sockets, are easily recognizable only in the point cloud from TLS and not identifiable in the other models.

The edges of objects are clearly identifiable in the case of the TLS point cloud. In the case of the other two systems, the edges are noisy and not easily recognizable (Figure 10 – Edge detail).

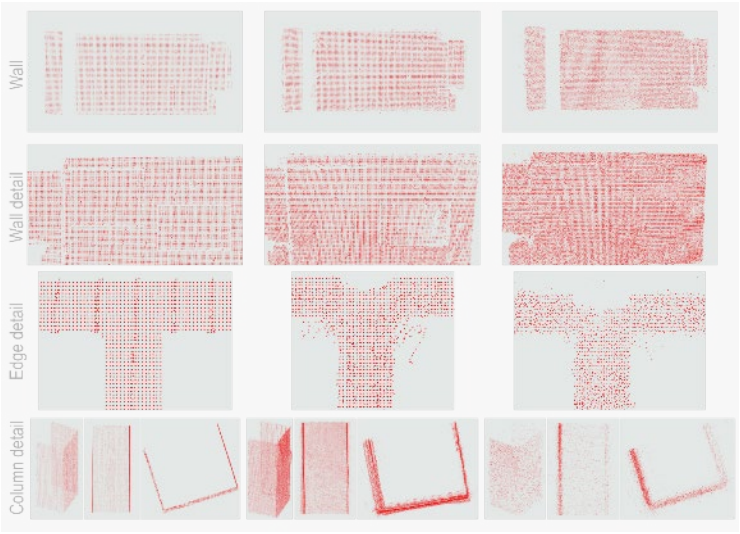

Figure 10
Segmentation-based evaluation of the results from TLS (left), Matterport Pro3 (middle), and the ZebGO (right)

The last row of Figure 10 shows a smaller object (observation pillar) from several views. The views presented show that the corners and edges are sharp only in the case of TLS. In other cases, the edges are noisy and hard to recognize. In addition, the pillar planes are slightly deformed due to the noise.

In addition, Table 6 shows the standard deviation of the plane estimations for each plane segment presented in Figure 10. The standard deviation is calculated based on the orthogonal distances from the regression plane of the inlier points for each plane. For the *column detail* (as shown in the bottom row of Figure 15), orthogonal regression was also employed following manual segmentation for estimating the plane parameters. Table 6 presents the average standard deviation of the plane estimation across all three planes. The standard deviation of the plane estimations for the two evaluated capturing systems is roughly twice as high as in the case of TLS.

Table 6
The standard deviation of the plane estimations

	std_{TLS} [mm]	**std_{Pro3}** [mm]	**std_{ZebGO}** [mm]
Wall	10	21	31
Wall detail	11	22	28
Edge detail	13	25	35
Column detail	8	23	32

4.3 Cloud-to-cloud Evaluation

The last evaluation was performed using the cloud-to-cloud method. This method considers all data, providing a more comprehensive view of the data's characteristics in some aspects, compared to individual control points or manually derived subsets from the entire point clouds. Before the assessment, the point clouds from the Matterport Pro3 and the GeoSLAM ZebGO were registered with the point cloud from TLS. The mutual transformation was performed in two steps in Leica Cyclone (Version 2023.1.0) software. Firstly, the course transformation was done by selecting identical points evenly distributed across the entire object. These selected points served as the basis for computing the initial transformation parameters. Next, the surface-based approach was used for the fine transformation, which is based on using overlapping surfaces in both point clouds. After the transformation, the CloudCompare (v2.12.4 (Kyiiv)) software was used for the third evaluation, where the *Cloud-to-Cloud Distance* function was applied to calculate the distances between the two clouds.

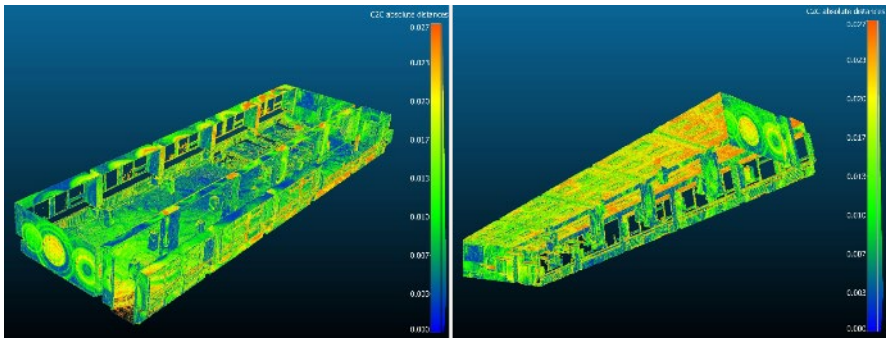

Figure 11
Cloud-to-cloud evaluation of the point cloud from the Matterport Pro3 camera

Figure 11 shows the result cloud-to-cloud comparison of the point cloud from the Pro3 camera with the TLS in two views, where the points are colored according to the computed distances. On the left side, a perspective view from above is shown, where the ceiling is removed for better visibility of the objects inside the first test scene. Figure 16 on the right depicts a reverse view from below, where the floor is removed vice versa.

On the right side of both images, a color scale is shown for the calculated distances, where the values are displayed in mm. The difference values varied from 0 to 30 mm for the whole point cloud. The most significant differences were achieved in the ceilings and some parts of the walls. In addition, it is also possible to notice the phenomenon that can often be encountered in the case of laser scanners with the phase-shift principle for distance measurement when parallel circles appear on straight walls [17].

Figure 12 shows the cloud-to-cloud evaluation of the point cloud from the ZebGO scanner from the same views as in the case of the point cloud from the Matterport Pro3. In this case, the distance between the TLS point cloud and the ZebGO point cloud varied from 0 to approximately 50 mm. The most significant differences were in the area of individual columns' side walls and the part of the ceiling. The differences in other parts of the object were below 30 mm.

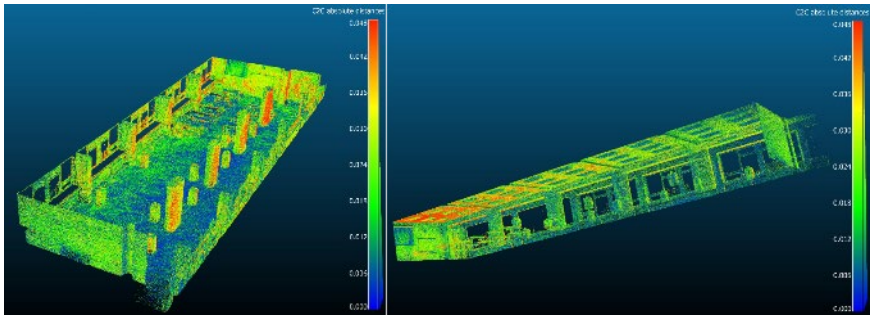

Figure 12
Cloud-to-cloud evaluation of the point cloud from the ZebGO scanner

5 Discussion

Three approaches were used to evaluate the selected systems. First was the control point approach. The test of the Matterport system with a 360° camera involved capturing several models with varying spacing distances between neighboring positions of the instrument. The comparison results revealed that the average root mean square (RMS) for models with 1.5 m spacing was 115 mm, while for models with 3 m spacing, it was 121 mm, and for models with 5 m spacing, it was 149 mm. Notably, the first test scene exhibited the worst results, possibly due to its size, variety, and complexity.

The evaluation of Matterport models captured with the Pro3 LIDAR camera followed a similar process as the 360° camera models. Notably, the differences between the TLS data and the Matterport models were consistently below 24 mm, confirming the apriori accuracy defined by the manufacturer. The Root Mean Square (RMS) error remained below 16 mm. Interestingly, the Pro3 camera's negligible differences between models with different spacing between the positions of the instrument can be attributed to its built-in LIDAR sensor. The last system evaluated was the handheld scanner GeoSLAM ZebGO, where the average RMS error for this method reaches 22 mm.

The following outcomes were affirmed through the second evaluation approach, which was segmentation-based. All two systems successfully captured larger walls,

rendering them easily visible and identifiable in the resulting point clouds. When it comes to smaller objects, the Pro3 has the ability to recognize them (for instance, a whiteboard), but it has difficulty with edge recognition. The ZebGO, on the other hand, struggles to identify these smaller objects at all. Only the point cloud produced by the TLS allows for easy recognition of finer details such as clocks and electrical sockets. Both the Pro3 and ZebGO display noisy edges, which complicates recognition. Besides what was previously mentioned, the evaluation also included the calculation of average standard deviations for plane estimations for each system. The results were as follows: 10.5 mm for TLS, 22.8 mm for the Pro3, and 31.5 mm for the ZebGO.

Regarding the Matterport system, which employs a 360° camera for capturing, its performance is significantly influenced by the camera orientation during the data acquisition. Additionally, the accuracy of the captured object depends on the number of images covering the given area. On the other hand, when using the Pro3 camera for capturing, the resulting accuracy is higher.

As for the GeoSLAM ZebGO, the results primarily hinge on how well the scanner is handled during the scanning process. The number of closed loops in the measured object and the frequency of area remeasurement also play a crucial role in determining the accuracy of the results.

Conclusions

This paper conducts a comparative study of several 3D data acquisition systems. These include, Matterport's system that utilizes 360° photos, the Matterport Pro3 LIDAR camera, and the GeoSLAM's handheld scanner ZebGO. These systems are compared against survey-grade TLS point clouds gathered from four distinct test sites. The article employs three primary evaluation approaches for these scanning systems: the control point approach, which compares segmented parts of the point cloud, and the cloud-to-cloud approach.

The evaluation showed, as anticipated, that point clouds from TLS have a higher geometric accuracy than the other systems. In addition, the point clouds from the evaluated systems tended to be noisier (especially in the case of the handheld scanner GeoSLAM ZebGO), and the detection of corners and edges of smaller objects could be challenging or even impossible. On the contrary, TLS needs more planning, and the measurement process is more time-consuming. Nevertheless, the disadvantages of the compared systems could be partly eliminated by repeated measurements or post-processing (e.g., noise filtering).

Overall, TLS offers the highest accuracy, making it ideal for detailed documentation of complex or large indoor spaces and heritage sites. The handheld GeoSLAM ZebGO provides a good compromise between mobility and accuracy for rapid modeling but lacks TLS-level detail. Matterport with a 360° camera suits quick visual capture of small to medium areas, though its geometric accuracy is limited.

The Pro3 LiDAR camera improves on this with better accuracy, supporting basic 3D modeling in larger or more complex spaces.

By examining and comparing the three different scanning systems, we demonstrated their advantages and disadvantages, in terms of technical and practical aspects, which can help when selecting an optimal system for specific purposes.

Acknowledgments

This work was supported by the Slovak Research and Development Agency under the Contract no. APVV-18-0247.

This publication was created with the support of the Scientific Grant Agency of the Ministry of Education, science, research and sport of the Slovak Republic and the Slovak Academy of Sciences for the project VEGA-1/0272/22.

Funded by the EU NextGenerationEU through the Recovery and Resilience Plan for Slovakia under the project No. 09I03-03-V05-00005.

References

[1] Ľ. Kovanič, M. Štroner, P. Blistan, R. Urban, and R. Boczek, "Combined ground-based and UAS SfM-MVS approach for determination of geometric parameters of the large-scale industrial facility – Case study," *Measurement*, Vol. 216, p. 112994, Jul. 2023, doi: 10.1016/j.measurement.2023.112994

[2] M. Jarząbek-Rychard and H.-G. Maas, "Modeling of 3D geometry uncertainty in Scan-to-BIM automatic indoor reconstruction," *Autom. Constr.*, Vol. 154, p. 105002, Oct. 2023, doi: 10.1016/j.autcon.2023.105002

[3] M. Kellner, B. Stahl, and A. Reiterer, "Reconstructing Geometrical Models of Indoor Environments Based on Point Clouds," *Remote Sens.*, Vol. 15, No. 18, p. 4421, Sep. 2023, doi: 10.3390/rs15184421

[4] J. Erdélyi, R. Honti, T. Funtík, P. Mayer, and A. Madiev, "Verification of Building Structures Using Point Clouds and Building Information Models," *Buildings*, Vol. 12, No. 12, p. 2218, Dec. 2022, doi: 10.3390/buildings12122218

[5] F. Bosché, M. Ahmed, Y. Turkan, C. T. Haas, and R. Haas, "The value of integrating Scan-to-BIM and Scan-vs-BIM techniques for construction monitoring using laser scanning and BIM: The case of cylindrical MEP components," *Autom. Constr.*, Vol. 49, pp. 201-213, Jan. 2015, doi: 10.1016/j.autcon.2014.05.014

[6] D. Bianculli and Humphries, *Application of Terrestrial Laser Scanner in Particle Accelerator and Reverse Engineering Solutions*. 2016, doi: 10.13140/RG.2.2.12345.36967

[7] N. A. B. Hariffin, M. H. B. Razali, L. C. Luh, S. A. Sulaiman, and M. B. M. Hashim, "The Suitability of Matterport for Building Parcel Dimension

Survey," in *2023 IEEE 13th International Conference on System Engineering and Technology (ICSET)*, Shah Alam, Malaysia: IEEE, Oct. 2023, pp. 239-244, doi: 10.1109/ICSET59111.2023.10295134

[8] V. Lehtola *et al.*, "Comparison of the Selected State-Of-The-Art 3D Indoor Scanning and Point Cloud Generation Methods," *Remote Sens.*, Vol. 9, No. 8, p. 796, Aug. 2017, doi: 10.3390/rs9080796

[9] J. Jung, S. Yoon, S. Ju, and J. Heo, "Development of Kinematic 3D Laser Scanning System for Indoor Mapping and As-Built BIM Using Constrained SLAM," *Sensors*, Vol. 15, No. 10, Art. no. 10, Oct. 2015, doi: 10.3390/s151026430

[10] B. Sirmacek, Y. Shen, R. Lindenbergh, S. Zlatanova, and A. Diakite, "Comparison of ZEB1 and Leica C10 indoor laser scanning point clouds," *ISPRS Ann. Photogramm. Remote Sens. Spat. Inf. Sci.*, Vol. III-1, pp. 143-149, Jun. 2016, doi: 10.5194/isprs-annals-III-1-143-2016

[11] G. Vosselman and H.-G. Maas, *Airborne and Terrestrial Laser Scanning.*, 1st ed., Vol. 1 in 1, Vol. 1. 2010

[12] "How Matterport Works | Matterport," How Matterport Works | Matterport. Accessed: Feb. 09, 2024 [Online] Available: https://matterport.com/how-it-works

[13] "Cortex AI | Matterport." Accessed: Feb. 09, 2024 [Online] Available: https://matterport.com/cortex-ai

[14] I. MacPherson, R. F. Murray, M. S. Brown, R. F. Murray, and M. S. Brown, "A 360° Omnidirectional Photometer using a Ricoh Theta Z1," *Color Imaging Conf.*, Vol. 30, pp. 124-128, Nov. 2022, doi: 10.2352/CIC.2022.30.1.23

[15] "GeoSLAM," ZEB Go Handheld 3D Scanner: Laser Scanning for Everyone. Accessed: Feb. 09, 2024 [Online] Available: https://geoslam.com/solutions/zeb-go/

[16] R. Honti, J. Erdélyi, and A. Kopáčik, "Semi-Automated Segmentation of Geometric Shapes from Point Clouds," *Remote Sens.*, Vol. 14, No. 18, p. 4591, Sep. 2022, doi: 10.3390/rs14184591

[17] P. Dorninger, C. Nothegger, N. Pfeifer, and G. Molnár, "On-the-job detection and correction of systematic cyclic distance measurement errors of terrestrial laser scanners," Vol. 2, No. 4, pp. 191-204, Dec. 2008, doi: 10.1515/JAG.2008.022